Ion Solvation Engineering: How to Manipulate the Multiplicity of the Coordination Environment of Multivalent Ions

Artem Baskin* and David Prendergast

Joint Center for Energy Storage Research, Molecular Foundry, Lawrence Berkeley National Laboratory, Berkeley, California 94720, United States

E-mail: abaskin@lbl.gov

Abstract

Free energy analysis of solvation structures of free divalent cations, their ion-pairs and neutral aggregates in low dielectric solvents reveals the multiplicity of thermodynamically stable cation solvation configurations and identifies the micro- and macroscopic factors responsible for this phenomenon. Specifically, we show the role of ion-solvent interactions and solvent mixtures in determining the cation solvation free energy landscapes. We show that it is the entropic contribution of solvent degrees of freedom that is responsible for the solvation multiplicity, and the mutual balance between enthalpic and entropic forces or their concerted contributions is what ultimately defines the most stable ion solvation configuration and creates new ones. We show general consequences of ion solvation multiplicity on thermodynamics of complex electrolytes, specifically in the context of homogeneous or interfacial charge transfer. Identified factors and their interplay provide a pathway to formulation of solvation design rules that can be used to control bulk solvation, interfacial chemistry and charge transfer. Our findings also suggest experimentally testable predictions.

Graphical TOC Entry

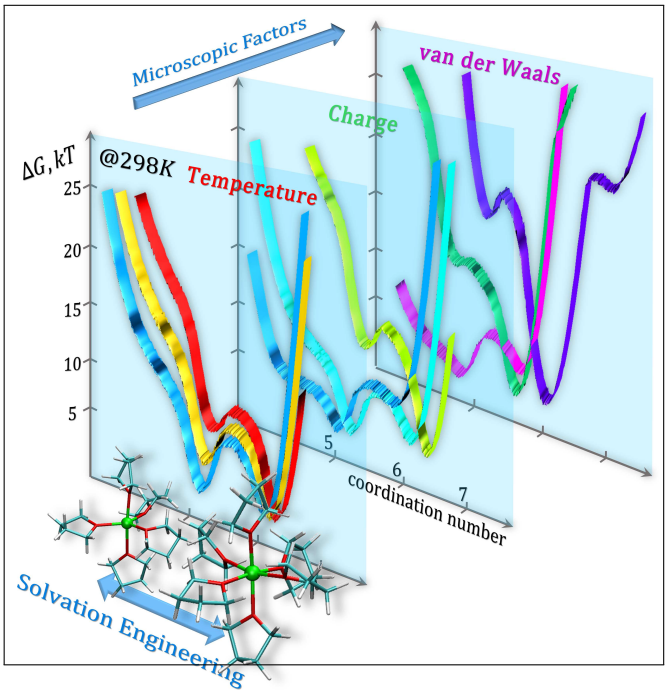

The science of solvation is at the heart of efforts towards the synthesis and design of a new generation of multivalent ion-based energy storage technologies.[1,2] In the bulk electrolytes, structural and dynamical aspects of ion solvation dictate chemical reactivity via solvent-specific redox potentials largely determined by solvation energies of reacting species. Processes of ion (de)solvation also control the interfacial chemistry,[3] charge transfer kinetics and transport properties, especially in solid[4] and polymer electrolytes[5] and ion-conducting membranes.[6,7] The energetics of ion solvation and the competition between enthalpic and entropic factors ultimately define the bulk and interfacial speciation which, in turn, defines the conductivity of electrolytes and stability of electrochemical interfaces. However, "taming" the complexity of solvation phenomena remains a formidable challenge and we are still far from taking full advantage of the opportunities this complexity grants.

There have been multiple attempts to benefit from manipulations with solvation of ionic species. The suppression of the solvent electrochemical activity in "water-in-salt" electrolytes[8,9] is an excellent example of gaining extra stability in conventional electrolytes with ions whose solvation shells are dramatically altered. Another example is the placement of charged functionalities in polymer backbones that enables tailoring the solvation cage environment and thereby offering efficient control over the conductivity and selectivity of such membranes.[10] In the field of multivalent cations and molecular anions in organic and aprotic solvents we see further evidence of the benefits that manipulation with ion solvation may provide: (1) electrolytes with mixed anions with different cation coordination strengths that enable decoupling cathodic and anodic processes to reduce corresponding overpotentials and suppress unwanted side reactions,[11] (2) tuning the anion-solvent interactions as well as the anion shapes,[12,13] and (3) in surface passivation assisted by neutral salt associates.[14] However, further progress is hindered by the lack of a molecular level understanding of related phenomena. Specifically, divalent cations salts in low dielectric solvents demonstrate a non-trivial concentration dependence of molar ionic conductivity. Spectroscopic and electrochemical probing reveals the unusual promotion of cations fully solvated by solvents at higher concentrations as opposed to predominant neutral aggregates forming in diluted electrolytes.[15,16] The relative anion and solvent donor numbers, the configurational flexibility of solvent, enhanced ionicity caused by formation of neutral or charged salt complexes[17,18] are proposed origins of these anomalous effects. Despite significant progress, these rationales are difficult to convert into a practical manual to meet specific metrics for design of new electrolytes, and many open questions remain.

Recently, using advanced free energy sampling techniques and the time-averaged continuous definition of coordination number as a metric to characterize solvation structures we predicted that some solvents[19] may support multiple (e.g., five- and six-fold) thermodynamically stable solvation configurations of cations. Moreover, in contrast to singular stable solvent coordinations resulting from simulations employing cluster analysis based on hybrid quantum chemistry and polarizable continuum modeling (QM-PCM) paired with regular molecular dynamics (MD), the free energy analysis revealed that the multiplicity of solvation structures of monoatomic cations or, as in the case of Zn^{2+}, the ability to accommodate a continuum of solvation configurations degenerate in free energies (Fig. S2), is an important microscale descriptor and could be a general feature of many electrolytes. The existence of multiple stable ion coordinations in solutions provides a channel to affect the reactivity of electrolytes due to the direct connection between ion solvation free energies and their redox potentials. The solvation multiplicity may also imply a significant difference between electronic properties of polyatomic solutes with distinctly different solvation environments.[20] Depending on ones needs - facilitating either reduction or oxidation of ions - the promotion of populations of lower or higher coordinated states, respectively, may be beneficial. Being able to switch between multiple solvation configurations would grant additional power to control bulk and interfacial speciation in electrolytes and allow us operate at the level of specificity that nature employs to turn subtle differences in alkali cations solvation into efficient and robust mechanisms in living cells.

However, before formulating principles of engineering solvation for multivalent ion electrolytes, we need to address several important questions. First, as the multiplicity of solvation structures of multivalent cations seems a general feature, it remains largely unclear what its origin is and what micro- and macroscopic factors can influence it. As evidenced by many experimental and theoretical studies, fully solvent solvated cations are rather an exception for multivalent aprotic electrolytes which instead exhibit many forms of ion-pairs and neutral aggregates. Therefore, the second question becomes: does the solvation multiplicity extend to the ions pairs, and if so, then what are the characteristics of their solvation dynamics (e.g., minimum free energy pathways, kinetic barriers, etc.)? Finally, as the energetics of solvation defines the thermodynamic population of ionic species, how does the multiplicity of solvation influence the equilibrium speciation of charged complexes, especially in low permittivity solvents at finite salt concentrations?

From a theoretical standpoint, controlling solvation implies control over interatomic interactions and molecular degrees of freedom. Therefore, general principles of engineering solvation should be then formulated in terms of short and long range interactions and enthalpic and entropic factors. To provide practical guidance we focus herein on the role of *temperature*, and *Coulomb* and *van der Waals forces* as a way to modulate (non)specific ion-ion and ion-solvent interactions. We also consider the *mixing of solvents* as an additional way

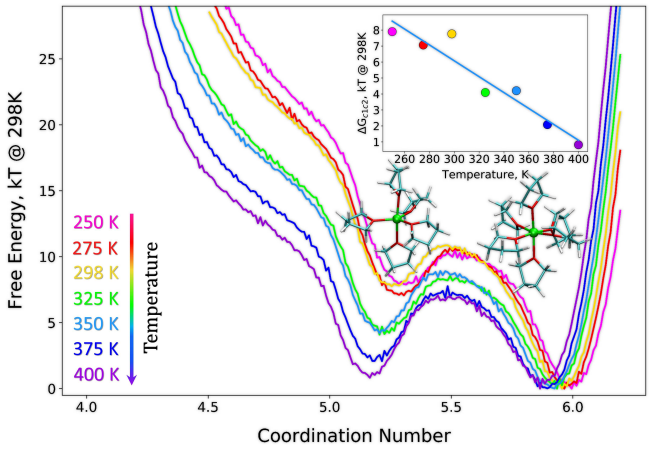

Figure 1: Temperature dependence of solvation structure of Mg^{2+} in tetrahydrofuran (THF). 1D free energies (in kT units) as functions of coordination numbers (number of oxygens of THF's molecules) for various temperatures (250 K to 400 K) are shown by colors. Dominant 6-fold and minor 5-fold configuration structures are shown. Inset shows the temperature dependence of the difference of free energies of five- and six-fold coordination states $\Delta G_{c_1c_2}(T) = G_{c1}(T) - G_{c2}(T)$ (colored dots) and the linear fit (blue line).

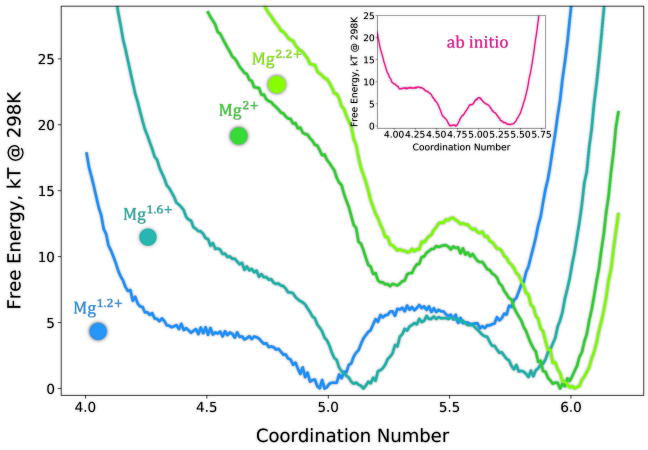

Figure 2: Dependence of solvation structures of Mg-cation in THF on the effective cation charge at $T = 298\,K$. 1D free energies (in kT units) as functions of coordination numbers (number of oxygens of THF's molecules) for various charges of Mg-cation (+1.2 to +2.2) are shown by colors. 1D ab initio free energy dependence for Mg^{2+} at $T = 298\,K$ in THF[19] is shown in the inset.

to affect the solvation environment. To illustrate these factors we consider $MgTFSI_2$ in tetrahydrofuran (THF) and diglyme (G2) electrolytes as important benchmark and widely studied systems,[21–30] to showcase various facets of solvation phenomenon. To properly describe the entropic contribution of the solvation and kinetic barriers we perform free energy analysis[31,32] using the metadynamics protocol as an advanced sampling technique[33,34] in the framework of classical MD paired with QM-PCM calculations (see the SI for details). We define the ion coordination number (CN) with respect to species of interest and the ion-ion distance as collective variables (CVs) used to compute 1D and 2D free energy surfaces.

We start by analyzing the temperature dependence of solvation structure of Mg^{2+} ion in THF (see SI for details). Previously, it was found[19] that Mg^{2+} demonstrates multiplicity of stable solvation configurations in THF. In the low concentration limit, our classical free energy sampling reveals that the lower 5-fold coordinated state becomes more stable with increasing temperature (see Table S2) as shown in Fig. 1. This observation highlights the role of entropy in stabilization of lower coordinated states that compensates their enthalpy loss. Further analysis requires the proper partitioning of the enthalpy and entropy contributions.[35] Assuming that neither enthalpy nor entropy depend explicitly on temperature, we approximate the temperature dependence of the free energy difference between stable five- and six-fold configurations as $\Delta G_{c_1c_2}(T) = \Delta H_{c_1c_2} - T\Delta S_{c_1c_2}$, where c_1 and c_2 correspond to the lower and higher coordination states, respectively. The linear fit (see inset Fig. 1) shows that this approximation is reasonable ($R^2 = 0.914$) and gives $\Delta G_{c_1c_2}(T)[\text{kcal/mol}] = 12.4279 - 0.02943\,\text{T}$.

At room temperature, $\Delta H_{c_1c_2} = 13.282\,\text{kcal/mol}$ and $\Delta S_{c_1c_2} = 29.41\,\text{cal/mol}\cdot\text{K}$ implying that the enthalpy of the lower coordinated state, c_1, is less stable (less negative), as we might expect from electrostatics, while the entropy of the same state is higher (more positive). There are two other effects associated with the temperature dependence of $\Delta G_{c_1c_2}$. As classical free energy sampling predicts, the lower coordinated state c_1 becomes not only more populated with temperature increase but also more stable as the kinetic barrier $\Delta G^{\dagger}_{c_1}$ that separates c_1 from c_2 increases (see Figures S3, S4) as well. Accordingly, the reverse kinetic barrier $\Delta G^{\dagger}_{c_2}$ decreases albeit not as fast as $\Delta G^{\dagger}_{c_1}$ does. These observations imply that entropy influences not only the mutual populations of coordination states but also the dynamics of ion solvation. Another interesting feature of the temperature dependence of solvation structures of the Mg^{2+} ion in THF is the monotonic shift of $\Delta G(CN)$ to the lower values of CN. This could be explained as the effects of anharmonicity of the Mg^{2+} - solvation sphere potential. At higher temperatures, less solvent molecules spends time inside the solvation sphere of a fixed radius.

Even though the control over temperature provides a macroscopic way to influence the balance between enthalpic and entropic forces, it has a limited potential to control ions solvation environment, since temperature is normally set externally. In the following sections we focus on microscopic factors that may control ion solvation configurations, specifically on those that define the chemistry of electrolytes itself. To this goal, we consider how electrostatic interactions and the charge of the cation can impact the multiplicity of solvation and the ultimate population of various ion coordination states. So far we tacitly assumed that the Mg-cation bears the full +2 charge. However, the polarization of

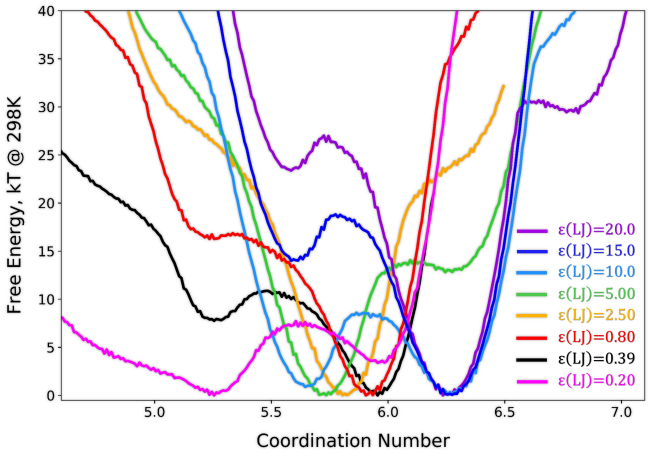

Figure 3: Dependence of the solvation structure of "effective" Mg cation in THF on the depth of vdW interaction between Mg and oxygens of THF. The charge of Mg cation is set as 2+ and the temperature is 298 K. Off-diagonal elements ε_{vdW}(Mg-O) = $\sqrt{\varepsilon_{\mathrm{vdW}}(\mathrm{Mg})\varepsilon_{\mathrm{vdW}}(\mathrm{O})}$ were set at 0.2, 0.39, 0.8, 2.50, 5.0, 10.0, 15.0, 20.0 kcal/mol as indicated by colors. ε_{vdW}(Mg-O) = 0.39 kcal/mol (black curve) is the original value.[19]

the ion, the covalency, the ionicity of the ion-solvent bonding, the specific environment or presence of interacting species[36] all affect the localization of the charge and thus the Coulomb interactions. Being motivated by the comparison between classical (fixed charge) and *ab initio* free energy samplings,[19] here we explore the role of Coulombic forces by tuning the "effective" charge of the Mg-cation in bulk THF and evaluate its free energy surface as a function of cation coordination number. In Fig. 2 we show the results of calculations. *Ab initio* modeling predicts (see inset Fig. 2) the lower and higher coordinated states to be almost degenerate in free energies whereas classical sampling with +2 charge on the Mg-cation results in a difference of ca. 8 kT at room temperature. However, when the cation charge is reduced by 20 % ($Mg^{1.6+}$) the 5-fold coordinated state becomes significantly stabilized and the classical sampling yields a free energy surface almost identical to that of *ab initio* umbrella sampling. Bader charge analysis on the Mg-cation in *ab initio* calculations also suggests that its charge is less than +2. Further "discharging" ($Mg^{1.2+}$) destabilizes the 6-fold coordinated state and makes coordination of the Mg-cation practically unimodal with its 5-fold coordination. On the other hand, promoting cation hardness with some extra charge ($Mg^{2.2+}$) clearly shows the enhancement of enthalpic forces and stabilization of 6-fold coordination state (see Table S3). This analysis shows that both the population of different solvation configurations and the dynamics of solvation are very sensitive to the state of "effective" charge of cations. Therefore, by choosing a coordinating solvent by its ability to hybridize electronically with a cation could be a way to exercise and accomplish control over ion solvation environment.

Next we explore the role of van der Waals (vdW) interactions in defining ion solvation free energy profiles.

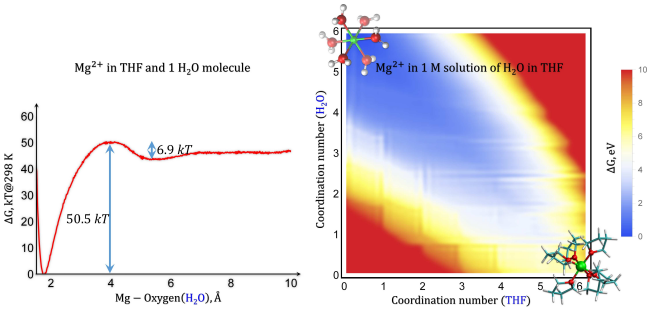

Figure 4: Free energy analysis of solvation structure of Mg^{2+} in a mixture of THF and water. Left: 1D free energy profile as a function of Mg^{2+} - water molecule distance in bulk THF. Right: 2D free energy surface with respect to Mg-cation coordination with water and THF molecules in 1 M solution of water in THF. Structures of Mg-cation six fold coordinated with water and with THF are shown. The charge of Mg cation is set as 2+ and the temperature is 298 K.

Specifically, we focus on the ion-solvent vdW interactions that along with Coulomb potentials largely determine ion solvation free energies and ion-solvent radial distribution functions.[37] We analyze how the depth of the vdW interaction between an "effective" Mg^{2+} ion and oxygen atoms of THF affects the multiplicity of solvation while keeping the equilibrium vdW interatomic distance fixed at the original value as well as the charge 2+ and temperature at 298 K (see SI for details). The dependence of the ion solvation configurations on the vdW radius of ions in water was previously studied.[38] In Fig. 3 we see that the variation of vdW parameters has a non-trivial impact on the solvation structure of the "Mg"-ion and it changes not only the values of optimal coordination numbers but also the number of stable solvation configurations. Specifically, the increase of $\varepsilon_{\mathrm{vdW}}$(Mg-O) from its original value of 0.39 kcal/mol (black curve) first destabilizes the lower coordinated state making it finally disappear (Fig. 3 red and orange curves, respectively) while shifting down the value of the most stable coordination. At $\varepsilon_{\mathrm{vdW}}$(Mg-O) $\simeq$ 5 kcal/mol (green curve) a new higher coordination state appears and what used to be a higher coordinated state becomes now a new lower one (see Figure S5). Further increase of $\varepsilon_{\mathrm{vdW}}$(Mg-O) stabilizes this new higher coordination state ($CN \approx 6.35$) and depopulates states at $CN \approx 5.6$ (green, lightblue and blue curves, respectively). Eventually, sufficiently high values of $\varepsilon_{\mathrm{vdW}}$(Mg-O) create a third stable coordination (violet curve). On the other hand, $\varepsilon_{\mathrm{vdW}}$(Mg-O) values smaller than 0.39 kcal/mol promote a lower coordinated state at $CN \approx 5.2$ (magenta curve). The non-monotonic change of global minimum of $\Delta G(CN)$ as a function of $\varepsilon_{\mathrm{vdW}}$(Mg-O) reflects the competition between attractive ion-solvent interactions and the steric solvent-solvent repulsion, the enthalpy and entropy driven mechanisms of stabilization of solvation configurations.

Finally, we explore the effects of mixing solvents on the Mg-cation coordination. Specifically, we focus on a mixture of THF and water as even a trace amount of water was shown to greatly affect the performance

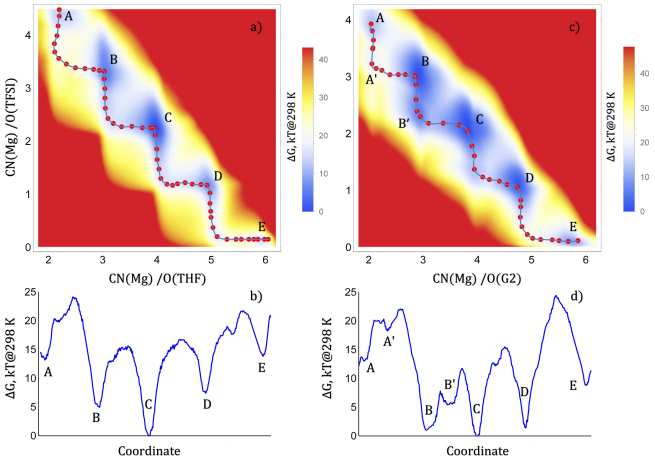

Figure 5: Free energy analysis of solvation structure of Mg-cation in $MgTFSI_2$ in THF (a,b) and G2 (c,d). a) 2D free energy profile as a function of the coordination of Mg-cation with respect to oxygens of THF and oxygens of TFSI-anions. b). The optimal path connecting the local minima (A-E). c) 2D free energy profile as a function of the coordination of Mg-cation with respect to oxygens of G2 and oxygens of TFSI-anions. d) The optimal path connecting the local minima (A-E). The secondary minima A' and B') are shown as well. Temperature is set at $T = 298\,K$.

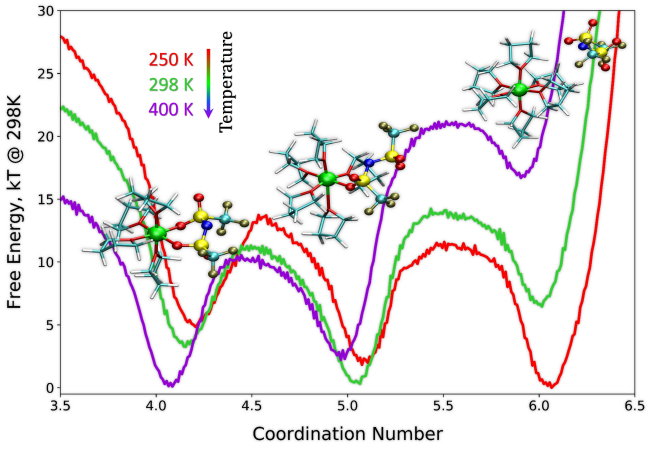

Figure 6: Temperature dependence of solvation structure of Mg-cation in its ion-pair $MgTFSI^+$ in THF. 1D free energy profile as a function of the coordination of Mg-cation with respect to oxygens of THF molecules. Profiles for $T = 250\,K$, $298\,K$, $400\,K$ are indicated by colors (red, green and violet, respectively). The stable structures of bidentate, monodentate and a solvent separated ion-pair are shown.

of non-aqueous electrolytes and kinetics of Mg deposition.[39] In Fig. 4 (left panel) we show the free energy profile of removal of one water molecule from Mg^{2+} ion in bulk THF. This analysis shows that the replacement of a water molecule in the Mg-cation solvation sphere by a THF molecule is very unlikely due to the high kinetic barrier of $\sim 50\,kT$. This exchange is also thermodynamically very unfavorable. Further analysis of solvation structure of Mg-cation in a mixture of water and THF reveals its extremely high hygroscopicity as 6-fold coordination with water is thermodynamically very stable as compared to configurations with few THF molecules in the solvation shell. This analysis highlights that Mg-cations work like an efficient scavenger that binds all available water molecules. On the other hand, this implies that these traces of water will be delivered to the interface and Mg-cations solvated with water may be a culprit for unwanted passivation of an electrode.

So far we considered the solvation structure of the Mg-cation in isolation assuming a very low concentration of salt. However, as mentioned above, in low dielectric solvents a significant population of neutral aggregates is expected. Herein, we consider the solvation structures of magnesium bis(trifluoromethanesulfonyl)imide ($MgTFSI_2$) in THF and diglyme (G2). In Fig. 5 we show 2D free energy surfaces of solvation structures of the Mg-cation in $MgTFSI_2$ resolved with respect to coordination with oxygens of the solvent molecules and oxygens of TFSI-anions. Our analysis largely confirms the "6-fold" rule of Mg coordination in both THF and G2 (Fig. 5 a,b and c,d, respectively) implying that the minima on the free energy surfaces correspond to combinations of coordination numbers that in total give six. Besides global minima that correspond to 4 oxygens of solvent and 2 oxygens from distinct TFSI-anions our analysis revealed other thermodynamically stable satellite configurations. Moreover, as predicted these configurations, whose populations are relatively significant as compared to the most stable one (less in THF, more in G2), are separated by substantial kinetic barriers ($\sim$ 10-15 kT). Solvent separated ion-pairs (SSIP) as well as di-bidentate configurations are also predicted to co-exist with other configurations (points A and E in Fig. 5 a and c). The lowest free energy pathways between the most stable solvation configurations of $MgTFSI_2$ in THF and G2 are shown as connected dots in Fig. 5 a and c and a parametric 1D plots in b and d. The key feature of these pathways are their staircase shape: the transformation of the Mg-cation solvation follows the path that suggests the sequential alternation of coordination with respect to solvent and then with respect to TFSI-anion(s) or vice versa but not a concerted change of coordination with respect to solvent and anions. The free energy profile of Mg-solvation in G2 is more complex and reveals more satellite structures. Specifically, it shows some secondary minima (e.g., A' and B') that do not follow the "6-fold" rule. These results are expected given the configurational flexibility of G2 molecules with multiple points of coordination with the Mg-cation.

We can extend the analysis of the multiplicity of solvation structures of the Mg-cation to its ion-pairs, specifically to $MgTFSI^+$ in THF. Here, the cation can be solvated by a solvent (THF) subsystem or the anion or both. The comparison of solvation environments of the Mg cation in $MgTFSI_2$ and $MgTFSI^+$ in THF shows the effects of TFSI anions that offer additional possibilities for the coordination. In Fig. 6 we show 1D free energy profiles with respect to the coordination of the Mg-cation with oxygens of THF molecules for $T = 250\,K$, $298\,K$ and $400\,K$. As our analysis shows, $MgTFSI^+$ in THF can exist in three configurations: sol-

vent separated ion-pair (SSIP) and mono- and bidentate contact ion-pairs. At room temperature, the monodentate configuration of $MgTFSI^+$ is the most stable one (compare with T=0 QM-PCM energies see Table S5 and Figure S1). The temperature dependence of solvation structure of the ion-pair reveals the same general trend as for an isolated Mg-cation. The increase of temperature results in entropy driven stabilization of lower coordinated states with respect to the solvent subsystem. SSIP can be also partially stabilized by the entropy gain due to the release of TFSI-anion. The 5-fold coordination state of the Mg-cation is eliminated due to the substantial enthalpy gain of coordination with the negatively charged TFSI-anion. These constructive effects of enthalpy and entropy gain favor the bidentate configuration of $MgTFSI^+$ at higher temperatures.

Despite the fact that our free energy analysis provides direct estimates of free energy differences between various coordination states, the predictions of average populations of these states at finite salt concentrations will be incorrect as they rely on single species properties at infinite dilution. However, our ability to theoretically and computationally predict speciation of ionic species at finite concentrations remain fairly limited. In the framework of statistical mechanics many approaches have been developed to study thermodynamics of ion-pairing. McMillan-Mayer and Kirkwood-Buff integral equations[40,41] were used to calculate concentration dependent activity coefficients. Classical density functional theory[42–44] and the reference interaction site model (RISM)[45,46] were used to calculate ion-ion and ion-solvent correlation functions. Ion-pairing in low permittivity solvents was also extensively studied using a wide range of multiscale computational methods. The improvements in predictions of structural and transport properties of such electrolytes were achieved with many-body polarizable force fields[47–49] or the ion charge renormalization method based on the semi-empirical "charge titration".[50] The predictions of equilibrium population of ionic species and the dissociation constants $\mathcal{K}_{dis}$ were recently improved using rescaling of dielectric constants of solvents caused by formation of solute dipolar aggregates ("redissociation").[17,18,51] However, these relatively cheap computational recipes suffer from the lack of consistency caused by problems of finding a self-consistent solution for coupled $\varepsilon_s = \varepsilon_s(\rho_i)$ and $\rho_i = \rho_i(\varepsilon_s)$, where ε_s and ρ_i are the dielectric permittivity of a solution and the ion-ion distribution function, respectively. Moreover, since the main focus of QM-PCM protocol based methods is on finding the energy difference ΔG_{dis} between bound and dissociated states, the discussion of equilibrium population of ion-pairs remains incomplete as the stability of that population implies kinetic barriers (Figure S6) that separate these states whose evaluation is beyond the scope of these methods.

From a fundamental standpoint, the observability of dissociation of ion-pairs in computational experiments is not just a problem of the force field or the electronic structure method. In systems with long-range interactions many-body correlations play a critical role in the processes of equilibration.[52,53] Therefore, accounting for the proper time and length scales in simulations is equally important for modeling of electrolytes. An electrolyte with an equilibrium ion-ion distribution function $\rho_i(r)$ can be characterized by Bjerrum $l_B = \frac{z_i z_j e^2}{\varepsilon_s kT}$ and Debye $l_D = \sqrt{\frac{\varepsilon_s kT}{4\pi e^2 \sum_j z_j^2 n_j}}$ mean-field length scales[54] that specify the dielectric and ionic screening, respectively. With the limited applicability to electrolytes with finite concentration, where both the dielectric constant ε_s and the ion concentrations n_j are not exactly known, these lengths are still foundational for studies of dynamics of ion-ion correlations[55] in a wide range of concentration regimes.[56–58] For monovalent ($z_j = 1$) electrolytes with nominal bulk concentration n at room temperature, $l_B[\text{Å}] = \frac{576.2}{\varepsilon_s}$ and $l_D[\text{Å}] = 0.341\sqrt{\frac{\varepsilon_s}{n[M]}}$. The comparison of these length scales with an average ion-ion distance $a_o[\text{Å}] = \frac{11.84}{\sqrt[3]{n[M]}}$ reveals that in low permittivity solvents and concentrations up to $1\,M$ the main mechanism of screening (see Figure S7) is the Debye screening. For example, in THF ($\varepsilon_s = 7$) $l_B = 82.3\,\text{Å}$, $l_D = 2.85\,\text{Å}$ and $l_D = 0.9\,\text{Å}$ as compared to $a_o = 25.5\,\text{Å}$ and $a_o = 11.84\,\text{Å}$ for $n = 0.1\,M$ and $1\,M$, respectively. These rough estimates show that even in classical MD simulations with unit cell sizes of 5 to 10 nm the thermodynamically stable ion dissociation is highly problematic. The relaxation time of the slow ions subsystem $\tau_{\rho_i \to \rho_i^{eq}}$[55,59] may be too long for the atomic simulations, and the effective mechanism of screening can be lost by the time when the majority of ions have already formed ion-pairs or neutral aggregates. It is worth noting that charge rescaling schemes (e.g., $q_i^{\text{eff}} = \frac{q_i}{\sqrt{\varepsilon_\infty}}$) only weaken the ionic screening.[60]

The conventional way to overcome the problem of finite simulation times is to use the free energy sampling. $\Delta G_{dis}(r_{ij} = a_o)$ (see Figure S6) of a ij-pair of ions would be then used to calculate the equilibrium population. However, when one defines a low-dimensional CV (e.g., a distance between i and j ions) for this sampling, the degrees of freedom of other ions are treated the same way as in the normal MD protocol, i.e., within a kT energy window. This entails the loss of the Debye screening as a factor of stabilization of ion dissociated states, and estimates of both ΔG_{dis} and kinetic barriers will be severely impaired. In Figure S8 we illustrate these ideas. The 2D free energy analysis of dissociation of $Mg(TFSI)_2$ in THF and diglyme at infinite dilution with mutual distances between Mg-cation and TFSI-anions as CVs shows that neither the full dissociation ($Mg^{2+}-2TFSI^-$, black lines a, d) nor the partial one ($MgTFSI^+-TFSI^-$, blue and red lines b, c and e, f) is stable. Therefore, ΔG_{dis} at the cation-anion distance of $r = 15\,\text{Å}$ cannot be used to evaluate the dissociation constant $\mathcal{K}_{dis}$ and the relative population of free ions versus bound configurations. This analysis also reveals multiple local free energy minima at shorter ion-

ion distances that correspond to mono- and bidentate $MgTFSI^+$ ion-pairs with either TFSI-anions or SSIP.

Having analyzed various factors that can shape solvation structures of cations in free or ion-pair forms, we can discuss the multiplicity of solvation from a general theoretical standpoint and show the main implications of this phenomenon for engineering ion solvation. The analysis of the temperature dependence of cation solvation structures w/o counterions (Fig. 1, Fig. 5 and Fig. 6), on the one hand, and ion-solvent (non)specific interactions (ion charge Fig. 2 and vdW interactions with the solvent Fig. 3), on the other, revealed the principal role of entropy in stabilization of low coordinated states. As we showed, it is instructive to separate the contributions from the solvent and from counterions. We can then hypothesize that the very existence of the ion solvation multiplicity crucially depends on the entropic contribution of solvent degrees of freedom (available at a given temperature) that is comparable to the enthalpic ion-solvent part of the solvation free energy. We then expect that in solvents with more thermally accessible degrees of freedom (high entropy solvents) that are directly affected by coordination with a cation, this multiplicity will be enhanced. The analysis of T-dependences of solvation structures of a free Mg-cation and the $MgTFSI^+$ ion-pair in THF suggests the same trend: higher temperature promotes lower coordination of the cation with the solvent. In the case of a free cation, entropy and enthalpy work against each other, and it is entropy that stabilizes the lower coordination. In the case of the $MgTFSI^+$ ion-pair, the multiplicity of solvation is promoted by the concerted contribution from both entropy and enthalpy. Here, the entropic gain due to the release of solvent molecules from the cation coordination sphere works along with the enthalpy gain due to the strong Coulomb attraction between counterions. We expect the same trends from neutral aggregates (e.g., $Mg(TFSI)_2$). The modulations of the cation hardness (ionic charge) and the solvent donor number (vdW) can be further used to tune or sample the relative stability and population of the coordination minima. Charge delocalization over the solvation sphere is also expected to greatly affect the solvation multiplicity.

Similar principles can be applied for engineering of solvation in other media. Specifically, the efficient segregation of solvation configurations of cations can be achieved in polymeric membranes with solvation cages tuned purposely to accommodate lower and higher cation coordination states. The design of such membrane functionalities should follow the same rules to achieve a proper balance between entropy and enthalpy of solvation.

Another important consequence of ion solvation multiplicity is related to the homogeneous or interfacial charge transfer. In the conventional Marcus theory, the contributing reactant and product states along a generalized solvent polarization coordinate are normally considered as single minima parabolas.[62–64] Depending on the overall exergonicity of the charge transfer reaction (tuned by e.g., an external bias) there are three distinct regimes: regular, when the solvent reorganization energy λ is higher than the overall free energy gain ΔG^0, barrierless, when $\lambda = \Delta G^0$, and inverted, when $\lambda < \Delta G^0$. As our study suggests, when solvent fluctuation effects are included explicitly,[65] besides ion-ion or ion-electrode distance coordinates, at least one of the contributing states should be properly represented by a multiminima surface. The immediate consequence of the interplay between crossing states with multiple minima is a new "mixed" regime, when increasing exergonicity leads to an inverted regime with respect to one minimum (e.g., higher coordination state) but remains in the regular regime with respect to another one (see Fig. 7). This may have an interesting impact on the processes of corrosion, especially with a surface coating that offers multiple ion solvation configurations, or homogeneous catalysis that involves complex ions.[66]

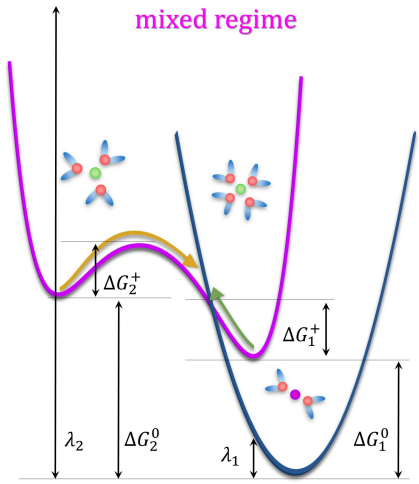

Figure 7: Illustration of the charge transfer kinetics in the case when one of the contributing states has two minima. Free energy gains ΔG_1^0 and ΔG_2^0, solvent reorganization energies λ_1 and λ_2, kinetic barriers $\Delta G_1^\dagger$ and $\Delta G_2^\dagger$ that correspond to the charge transfer to higher and lower coordination states of an ion, are shown respectively. Standard notations for ΔG and λ are used.[61] A mixed regime corresponds to a situation when $\lambda_1 < \Delta G_1^0$ but $\lambda_2 > \Delta G_2^0$.

Given the new perspectives that ion solvation multiplicity grants, it would be interesting to explore this phenomenology experimentally. Due to the sensitivity to the solvent dynamics around ions and ion-pairs of NMR,[67] dielectric relaxation[68] and anisotropy decay measurements with polarization-resolved IR spectroscopy,[69] we expect these experimental techniques paired with synthesis efforts on high entropy solvents or membranes to be appropriate tools to study predicted effects.

ASSOCIATED CONTENT

Supporting Information

A comprehensive description of (1) the general computational methodology used in this study, (2) the descrip-

tion of details of the regular classical molecular dynamics protocol, (3) the description of the regular ab initio molecular dynamics protocol, (4) the description of quantum chemistry calculations and the hybrid cluster/continuum polarizable model quantum chemistry protocol, (5) the description of the free energy sampling protocols (umbrella sampling and metadynamics) and the definition of the collective variables, (6) Mean-field Bjerrum and Debye screening lengths and details of the free energy analysis of $MgTFSI_2$ in THF and G2, (7) Parameters of the classical force fields and atomic charges, (8) equilibrium atomic structures of $MgTFSI^+$ ion-pairs in THF.

AUTHOR INFORMATION

Notes

The authors declare no competing financial interest.

Acknowledgments

This work was supported by the Joint Center for Energy Storage Research, an Energy Innovation Hub funded by the U.S. Department of Energy, Office of Science, Basic Energy Sciences. Portions of this work were supported by a User Project at The Molecular Foundry and its compute cluster (vulcan), managed by the High Performance Computing Services Group, at Lawrence Berkeley National Laboratory (LBNL), and portions of this work used the computing resources of the National Energy Research Scientific Computing Center, LBNL, both of which are supported by the Office of Science of the U.S. Department of Energy under contract no. DE-AC02-05CH11231.

References

(1) Trahey, L.; Brushett, F. R.; Balsara, N. P.; Ceder, G.; Cheng, L.; Chiang, Y.-M.; Hahn, N. T.; Ingram, B. J.; Minteer, S. D.; Moore, J. S. et al. Energy storage emerging: A perspective from the Joint Center for Energy Storage Research. *PNAS* **2020**, *117*, 12550–12557.

(2) Liang, Y.; Dong, H.; Aurbach, D.; Yao, Y. Current status and future directions of multivalent metal-ion batteries. *Nature Energy* **2020**, *ASAP*.

(3) Attias, R.; Salama, M.; Hirsch, B.; Goffer, Y.; Aurbach, D. Anode-Electrolyte Interfaces in Secondary Magnesium Batteries. *Joule* **2019**, *3*, 27–52.

(4) Zhao, Q.; Stalin, S.; Zhao, C.-Z.; Archer, L. A. Designing solid-state electrolytes for safe, energy-dense batteries. *Nat. Rev. Mater.* **2020**, *5*, 229–252.

(5) Choo, Y.; Halat, D. M.; Villaluenga, I.; Timachova, K.; Balsara, N. P. Diffusion and migration in polymer electrolytes. *Prog. Polym. Sci.* **2020**, *103*, 101220.

(6) Wang, L.; Zhao, Y.; Fan, B.; Carta, M.; Malpass-Evans, R.; McKeown, N. B.; Marken, F. Polymer of Intrinsic Microporosity (PIM) Films and Membranes in Electrochemical Energy Storage and Conversion: A Mini-Review. *Electrochem. Commun.* **2020**, *118*, 106798.

(7) Kushner, D. I.; Crothers, A. R.; Kusoglu, A.; Weber, A. Z. Transport phenomena in flow battery ion-conducting membranes. *Curr. Opin. Electrochem.* **2020**, *21*, 132–139.

(8) Suo, L.; Borodin, O.; Gao, T.; Olguin, M.; Ho, J.; Fan, X.; Luo, C.; Wang, C.; Xu, K. "Water-in-salt" electrolyte enables high-voltage aqueous lithium-ion chemistries. *Science* **2015**, *350*, 938–943.

(9) Chen, L.; Zhang, J.; Li, Q.; Vatamanu, J.; Ji, X.; Pollard, T. P.; Cui, C.; Hou, S.; Chen, J.; Yang, C. et al. A 63 m Superconcentrated Aqueous Electrolyte for High-Energy Li-Ion Batteries. *ACS Energy Lett.* **2020**, *5*, 968–974.

(10) Baran, M. J.; Braten, M. N.; Sahu, S.; Baskin, A.; Meckler, S. M.; Li, L.; Maserati, L.; Carrington, M. E.; Chiang, Y.-M.; Prendergast, D. et al. Design Rules for Membranes from Polymers of Intrinsic Microporosity for Crossover-free Aqueous Electrochemical Devices. *Joule* **2019**, *3*, 2968–2985.

(11) Connell, J. G.; Zorko, M.; Agarwal, G.; Yang, M.; Liao, C.; Assary, R. S.; Strmcnik, D.; Markovic, N. M. Anion Association Strength as a Unifying Descriptor for the Reversibility of Divalent Metal Deposition in Nonaqueous Electrolytes. *ACS Appl. Materials & Interfaces* **2020**, *12*, 36137–36147.

(12) Fiates, J.; Zhang, Y.; Franco, L. F. M.; Maginn, E. J.; Doubek, G. Impact of anion shape on Li+ solvation and on transport properties for lithiumâĂŞair batteries: a molecular dynamics study. *Phys. Chem. Chem. Phys.* **2020**, *22*, 15842–15852.

(13) Popov, I.; Sacci, R. L.; Sanders, N. C.; Matsumoto, R. A.; Thompson, M. W.; Osti, N. C.; Kobayashi, T.; Tyagi, M.; Mamontov, E.; Pruski, M. et al. Critical Role of Anion-Solvent Interactions for Dynamics of Solvent-in-Salt Solutions. *J. Phys. Chem. C* **2020**, *124*, 8457–8466.

(14) Nie, M.; Abraham, D. P.; Seo, D. M.; Chen, Y.; Bose, A.; Lucht, B. L. Role of Solution Structure in Solid Electrolyte Interphase Formation on

Graphite with $LiPF_6$ in Propylene Carbonate. *J. Phys. Chem. C* **2013**, *117*, 25381–25389.

(15) Chen, Y.; Jaegers, N. R.; Wang, H.; Han, K. S.; Hu, J. Z.; Mueller, K. T.; Murugesan, V. Role of Solvent Rearrangement on Mg2+ Solvation Structures in Dimethoxyethane Solutions using Multimodal NMR Analysis. *J. Phys. Chem. Lett.* **2020**, *11*, 6443–6449.

(16) Hahn, N. T.; Self, J.; Seguin, T. J.; Driscoll, D. M.; Rodriguez, M. A.; Balasubramanian, M.; Persson, K. A.; Zavadil, K. R. The critical role of configurational flexibility in facilitating reversible reactive metal deposition from borohydride solutions. *J. Mater. Chem. A* **2020**, *8*, 7235–7244.

(17) Self, J.; Wood, B. M.; Rajput, N. N.; Persson, K. A. The Interplay between Salt Association and the Dielectric Properties of Low Permittivity Electrolytes: The Case of $LiPF_6$ and $LiAsF_6$ in Dimethyl Carbonate. *J. Phys. Chem. C* **2018**, *122*, 1990–1994.

(18) Self, J.; Hahn, N. T.; Fong, K. D.; McClary, S. A.; Zavadil, K. R.; Persson, K. A. Ion Pairing and Redissociaton in Low-Permittivity Electrolytes for Multivalent Battery Applications. *J. Phys. Chem. Lett.* **2020**, *11*, 2046–2052.

(19) Baskin, A.; Prendergast, D. "Ion Solvation Spectra": Free Energy Analysis of Solvation Structures of Multivalent Cations in Aprotic Solvents. *J. Phys. Chem. Lett.* **2019**, *10*, 4920–4928.

(20) Widmer, D. R.; Schwartz, B. J. Solvents can control solute molecular identity. *Nature Chem.* **2018**, *10*, 910–916.

(21) Ha, S.-Y.; Lee, Y.-W.; Woo, S. W.; Koo, B.; Kim, J.-S.; Cho, J.; Lee, K. T.; Choi, N.-S. Magnesium(II) Bis(trifluoromethane sulfonyl) Imide-Based Electrolytes with Wide Electrochemical Windows for Rechargeable Magnesium Batteries. *ACS Appl. Mater. Interfaces* **2014**, *6*, 4063–4073.

(22) Kim, D. Y.; Lim, Y.; Roy, B.; Ryu, Y.-G.; Lee, S.-S. Operating Mechanisms of Electrolytes in Magnesium Ion Batteries: Chemical Equilibrium, Magnesium Deposition, and Electrolyte Oxidation. *Phys. Chem. Chem. Phys.* **2014**, *16*, 25789–25798.

(23) Lapidus, S. H.; Rajput, N. N.; Qu, X.; Chapman, K. W.; Persson, K. A.; Chupas, P. J. Solvation Structure and Energetics of Electrolytes for Multivalent Energy Storage. *Phys. Chem. Chem. Phys.* **2014**, *16*, 21941–21945.

(24) Shterenberg, I.; Salama, M.; Yoo, H. D.; Gofer, Y.; Park, J.-B.; Sun, Y.-K.; Aurbach, D. Evaluation of $(CF_3SO_2)_2N$-(TFSI) Based Electrolyte Solutions for Mg Batteries. *J. Electrochem. Soc.* **2015**, *162*, A7118–A7128.

(25) Rajput, N. N.; Qu, X.; Sa, N.; Burrell, A. K.; Persson, K. A. The Coupling between Stability and Ion Pair Formation in Magnesium Electrolytes from First-Principles Quantum Mechanics and Classical Molecular Dynamics. *J. Am. Chem. Soc.* **2015**, *137*, 3411–3420.

(26) Baskin, A.; Prendergast, D. Exploration of the Detailed Conditions for Reductive Stability of $Mg(TFSI)_2$ in Diglyme: Implications for Multivalent Electrolytes. *J. Phys. Chem. C* **2016**, *120*, 3583–3594.

(27) Kimura, T.; Fujii, K.; Sato, Y.; Morita, M.; Yoshimoto, N. Solvation of Magnesium Ion in Triglyme-Based Electrolyte Solutions. *J. Phys. Chem. C* **2015**, *119*, 18911–18917.

(28) Sa, N.; Rajput, N. N.; Wang, H.; Key, B.; Ferrandon, M.; Srinivasan, V.; Persson, K. A.; Burrell, A. K.; Vaughey, J. T. Concentration dependent electrochemical properties and structural analysis of a simple magnesium electrolyte: magnesium bis(trifluoromethane sulfonyl)imide in diglyme. *Phys. Chem. Chem. Phys.* **2016**, *6*, 113663–113670.

(29) Hu, J. Z.; Rajput, N. N.; Wan, C.; Shao, Y.; Deng, X.; Jaegers, N. R.; Hu, M.; Chen, Y.; Shin, Y.; Monk, J. et al. ^{25}Mg NMR and computational modeling studies of the solvation structures and molecular dynamics in magnesium based liquid electrolytes. *Nano Energy* **2018**, *46*, 436–446.

(30) Rajput, N. N.; Seguin, T. J.; Wood, B. M.; Qu, X.; Persson, K. A. Elucidating Solvation Structures for Rational Design of Multivalent Electrolytes - A Review. *Top Curr. Chem. (Z)* **2018**, *376:19*, 1–46.

(31) Beveridge, D. L.; DiCapua, F. M. Free Energy Via Molecular Simulation: Applications to Chemical and Biomolecular Systems. *Annu. Rev. Biophys. Chem.* **1989**, *18*, 431–492.

(32) Trzesniak, D.; Kunz, A.-P. E.; van Gunsteren, W. F. A Comparison of Methods to Compute the Potential of Mean Force. *ChemPhysChem* **2007**, *8*, 162–169.

(33) Laio, A.; Gervasio, F. L. Metadynamics - A Method to Stimulate Rare Events and Reconstruct the Free Energy in Biophysics, Chemistry and Material Science. *Rep. Prog. Phys.* **2008**, *71*, 126601.

(34) Barducci, A.; Bonomi, M.; Parrinello, M. Metadynamics. *Wiley Inter. Rev.: Comp. Mol. Sci.* **2011**, *1*, 826–843.

(35) Yu, H.; Karplus, M. A thermodynamic analysis of solvation. *J. Chem. Phys.* **1988**, *89*, 2366–2379.

(36) Legg, B. A.; Baer, M. D.; Chun, J.; Schenter, G. K.; Huang, S.; Zhang, Y.; Min, Y.; Mundy, C. J.; De Yoreo, J. J. Visualization of Aluminum Ions at the Mica Water Interface Links Hydrolysis State-to-Surface Potential and Particle Adhesion. *J. Am Chem. Soc.* **2020**, *142*, 6093–6102.

(37) Aqvist, J. Ion-water interaction potentials derived from free energy perturbation simulations. *J. Phys. Chem.* **1990**, *94*, 8021–8024.

(38) Roy, S.; Baer, M. D.; Mundy, C. J.; Schenter, G. K. Reaction Rate Theory in Coordination Number Space: An Application to Ion Solvation. *J. Phys. Chem. C* **2016**, *120*, 7597–7605.

(39) Connell, J. G.; Genorio, B.; Lopes, P. P.; Strmcnik, D.; Stamenkovic, V. R.; Markovic, N. M. Tuning the Reversibility of Mg Anodes via Controlled Surface Passivation by H_2O/Cl^- in Organic Electrolytes. *Chem. Mater.* **2016**, *28*, 8268–8277.

(40) McMillan, W. G.; Mayer, J. E. The Statistical Thermodynamics of Multicomponent Systems. *J. Chem. Phys.* **1945**, *13*, 276–305.

(41) Kirkwood, J. G.; Buff, F. P. The Statistical Mechanical Theory of Solutions. I. *J. Chem. Phys.* **1951**, *19*, 774–777.

(42) Tarazona, P.; Evans, R. A simple density functional theory for inhomogeneous liquids. *Mol. Phys.* **1984**, *52*, 847–857.

(43) Roth, R. Fundamental measure theory for hard-sphere mixtures: a review. *J. Phys.: Condens. Matter* **2010**, *22*, 063102.

(44) Hansen, J. P.; McDonald, I. R. *Theory of simple Liquids, 2nd ed.*; Academic Press, London, 1986.

(45) Hirata, F.; Rossky, P. J. An extended rism equation for molecular polar fluids. *Chem. Phys. Lett.* **1981**, *83*, 329–334.

(46) Kovalenko, A.; Hirata, F. Three-dimensional density profiles of water in contact with a solute of arbitrary shape: a RISM approach. *Chem. Phys. Lett.* **1998**, *290*, 237–244.

(47) Borodin, O. Polarizable Force Field Development and Molecular Dynamics Simulations of Ionic Liquids. *J. Phys. Chem. B* **2009**, *113*, 11463–11478.

(48) Luo, Y.; Jiang, W.; Yu, H.; MacKerell, A. D.; Roux, B. Simulation study of ion pairing in concentrated aqueous salt solutions with a polarizable force field. *Faraday Discuss.* **2013**, *160*, 135–149.

(49) Bedrov, D.; Piquemal, J.-P.; Borodin, O.; MacKerell, A. D.; Roux, B.; Schröder, C. Molecular Dynamics Simulations of Ionic Liquids and Electrolytes Using Polarizable Force Fields. *Chem. Rev.* **2019**, *119*, 7940–7995.

(50) Li, Z.; Robertson, L. A.; Shkrob, I. A.; Smith, K. C.; Cheng, L.; Zhang, L.; Moore, J. S.; Z, Y. Realistic Ion Dynamics through Charge Renormalization in Nonaqueous Electrolytes. *J. Phys. Chem. B* **2020**, *124*, 3214–3220.

(51) Self, J.; Fong, K. D.; Logan, E. R.; Persson, K. A. Ion Association Constants for Lithium Ion Battery Electrolytes from First-Principles Quantum Chemistry. *J. Electrochem. Soc.* **2019**, *166*, A3554–A3558.

(52) Balescu, R. Irreversible Processes in Ionized Gases. *Phys. of Fluids* **1960**, *3*, 52.

(53) Balescu, R. Binary Correlations in Ionized Gases. *Phys. of Fluids* **1961**, *4*, 85.

(54) Marcus, Y.; Hefter, G. Ion Pairing. *Chem. Rev.* **2007**, *38*, 4585–4621.

(55) Jasperse, J. R.; Basu, B. The dielectric function for the Balescu-Lenard-Poisson kinetic equationsa. *Phys. of Fluids* **1986**, *29*, 110.

(56) Keblinski, P.; Eggebrecht, J.; Wolf, D.; Phillpot, S. R. Molecular dynamics study of screening in ionic fluids. *J. Chem. Phys.* **2000**, *113*, 282–291.

(57) Fennell, C. J.; Bizjak, A.; Vlachy, V.; Dill, K. A.; Sarupria, S.; Rajamani, S.; Garde, S. Ion Pairing in Molecular Simulations of Aqueous Alkali Halide Solutions. *J. Phys. Chem. B* **2009**, *113*, 14837–14838.

(58) Coles, S. W.; Park, C.; Nikam, R.; Kanduč, M.; Dzubiella, J.; Rotenberg, B. Correlation Length in Concentrated Electrolytes: Insights from All-Atom Molecular Dynamics Simulations. *J. Chem. Phys. B* **2020**, *124*, 1778–1786.

(59) Balescu, R. *Equilibrium and Nonequilibrium Statistical Mechanics.*; John Wiley and Sons, 1975.

(60) Leontyev, I. V.; Vener, M. V.; Rostov, I. V.; Basilevsky, M. V.; Newton, M. D. Continuum level treatment of electronic polarization in the framework of molecular simulations of solvation effects. *J. Chem. Phys.* **2003**, *119*, 8024–8037.

(61) Wu, Q.; Van Voorhis, T. Direct Calculation of Electron Transfer Parameters through Constrained Density Functional Theory. *J. Phys. Chem. A* **2006**, *110*, 9212–9218.

(62) Schmickler, W. A theory of adiabatic electron-transfer reactions. *J. Electroanal. Chem.* **1986**, *204*, 31–43.

(63) Marcus, R. Tutorial on rate constants and reorganization energies. *J. Electroanal. Chem.* **2000**, *483*, 2–6.

(64) Gosavi, S.; Marcus, R. A. Nonadiabatic Electron Transfer at Metal Surfaces. *J. Phys. Chem. B* **2000**, *104*, 2067–2072.

(65) Roy, S.; Baer, M. D.; Mundy, C. J.; Schenter, G. K. Marcus Theory of Ion-Pairing. *J. Chem. Theory. Comput.* **2017**, *13*, 3470–3477.

(66) Parada, G. A.; Goldsmith, Z. K.; Kolmar, S.; Pettersson Rimgard, B.; Mercado, B. Q.; Hammarström, L.; Hammes-Schiffer, S.; Mayer, J. M. Concerted proton-electron transfer reactions in the Marcus inverted region. *Science* **2019**, *364*, 471–475.

(67) Hu, J. Z.; Jaegers, N. R.; Hu, M. Y.; Mueller, K. T. In situ and ex situ NMR for battery research. *J. Phys. Condensed Mat.* **2018**, *30*, 463001.

(68) Buchner, R.; Chen, T.; Hefter, G. Complexity in "Simple" Electrolyte Solutions: Ion Pairing in $MgSO_4$(aq). *J. Phys. Chem B* **2004**, *108*, 2365–2375.

(69) Bian, H.; Chen, H.; Zhang, Q.; Li, J.; Wen, X.; Zhuang, W.; Zheng, J. Cation Effects on Rotational Dynamics of Anions and Water Molecules in Alkali (Li^+, Na^+, K^+, Cs^+) Thiocyanate (SCN^-) Aqueous Solutions. *J. Phys. Chem B* **2013**, *117*, 7972–7984.